

# Direct Top Quark Production at Hadron Colliders as a Probe of New Physics

M. Hosch, K. Whisnant, and B.-L. Young  
Department of Physics and Astronomy  
Iowa State University  
Ames, Iowa 50011 USA

## Abstract

We examine the effect of an anomalous flavor changing chromomagnetic moment which allows direct top quark production (two partons combining into an unaccompanied single top quark in the s-channel) at hadron colliders. We consider both t-c-g and t-u-g couplings. We find that the anomalous charm quark coupling parameter  $\kappa_c/\Lambda$  can be measured down to  $.06 \text{ TeV}^{-1}$  ( $.009 \text{ TeV}^{-1}$ ) at the Tevatron with the Main Injector upgrade(LHC). The anomalous up quark coupling parameter  $\kappa_u/\Lambda$  can be measured to  $.02 \text{ TeV}^{-1}$  ( $.003 \text{ TeV}^{-1}$ ) at the Tevatron(LHC).

## Introduction

With the discovery of the top quark [1, 2], the long anticipated completion of the fermion sector of the standard model has been achieved. Its unexpected large mass in comparison with the other known fermions suggests that the top quark may play a unique role in probing new physics, and has prompted both theorists and experimenters alike to search for anomalous couplings involving the top quark. On the experimental side, the CDF [3, 4] and D0 [5] collaborations have begun to explore the physics of top quark rare decays [3]. On the theoretical side, a systematic examination of anomalous top quark interactions, in a model independent way, has been actively undertaken[6, 7].

One possible set of anomalous interactions for the top quark is given by the flavor-changing chromo-magnetic operators:

$$\frac{\kappa_u}{\Lambda} g_s \bar{u} \sigma^{\mu\nu} \frac{\lambda^a}{2} t G_{\mu\nu}^a + h.c. , \quad (1)$$

and

$$\frac{\kappa_c}{\Lambda} g_s \bar{c} \sigma^{\mu\nu} \frac{\lambda^a}{2} t G_{\mu\nu}^a + h.c. , \quad (2)$$

where  $\Lambda$  is the new physics scale,  $\kappa_c$  and  $\kappa_u$  define the strengths of the couplings, and  $G_{\mu\nu}^a$  is the gauge field tensor of the gluon. The investigation of these couplings is well motivated. Although these operators can be induced in the standard model through higher order loops, their effects are too small to be observable[8]. Therefore, any observed signal indicating these types of couplings is direct evidence for physics beyond the standard model.

It has been argued that the couplings in Eqs. (1) and (2) may be significant in many extensions to the standard model, such as supersymmetry (SUSY) or other models with multiple Higgs doublets [8, 9, 10, 11], models with new dynamical interactions of the top quark[12], and models where the top quark has a composite[13] or soliton[14] structure. In particular, Ref. [10] suggests that the supersymmetric contributions to a t-c-g vertex may be large enough to measure at a future hadron collider.

T. Han et. al.[15] have placed a limit on the top-charm-gluon coupling strength,  $\kappa_c$ , by examining the decay of the top quark into a charm quark and a gluon. They find an upper limit on  $\kappa_c/\Lambda$  of .43(.65)  $\text{TeV}^{-1}$  with(without) b-tagging for 200  $\text{pb}^{-1}$  of data at the Tevatron. If the c and u jets are not distinguished, their result applies equally well to  $\kappa_u/\Lambda$ , if one uses the up quark coupling alone, or to the sum, added in quadrature, when both are considered.

In this paper, we will examine these operators in a model independent way using direct top quark production at the Fermilab Tevatron and at the CERN LHC. In this scenario, a charm (or up) quark and a gluon from the colliding hadrons combine immediately to form an s-channel top quark, which then decays. The production of a single, unaccompanied top or anti-top quark is very small in the standard model. For simplicity, we consider couplings to the up quark and to the charm quark independently. We will take as our signal only the case where the top quark decays to a b quark and a W boson. While the  $t \rightarrow cg$  (or  $ug$ ) decay will occur in the presence of the anomalous couplings given in Eqs. (1) and (2), it is smaller than the  $t \rightarrow bW$

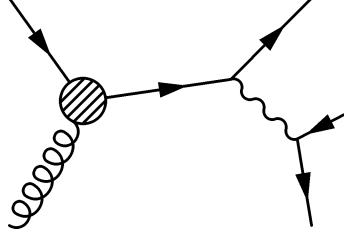


Figure 1: Feynmann diagram for direct top quark production and subsequent decay into  $bl\nu_l$

decay for  $\kappa/\Lambda \lesssim .75 \text{ TeV}^{-1}$ , and will have a negligible branching ratio for  $\kappa/\Lambda \lesssim .2 \text{ TeV}^{-1}$ . Given the existing upper bound of the anomalous coupling mentioned earlier [15],  $t \rightarrow bW$  will be the dominant decay mode of the top quark. Since the W boson decay into a charged lepton (electron or muon) and its corresponding neutrino has an identifiable signature, we consider only the  $t \rightarrow bW \rightarrow bl\nu_l$  decay for our signal. With the decays so chosen, we find that the backgrounds are manageable, as will be discussed in detail later.

## Direct Top Quark Production

We have calculated tree level cross sections for direct top quark production,  $p\bar{p} \rightarrow t \rightarrow bW^+ \rightarrow bl^+\nu_l$ , using the flavor-changing chromomagnetic moments in Eqs. (1) and (2) (see Fig. 1). The  $l^+$  in this process is either a positron or an anti-muon, and  $\nu_l$  is its corresponding neutrino. We also included direct anti-top production in our calculation ( $p\bar{p} \rightarrow \bar{t} \rightarrow \bar{b}W^- \rightarrow \bar{b}l^-\bar{\nu}_l$ ). The parton cross section for direct top(or anti-top) production is given by:

$$d\sigma = \frac{1}{4} \frac{1}{(4\pi)^5} \frac{\hat{s} - M_{l,\nu_l}^2}{\hat{s}^2} |\overline{\mathcal{M}}|^2 d\Omega_b d\Omega_l dM_{l,\nu_l}^2, \quad (3)$$

where the spin averaged squared matrix element is

$$|\overline{\mathcal{M}}|^2 = \frac{256\pi^3 \alpha_2^2 \alpha_s \kappa_{c(u)}^2}{3} \frac{\hat{s} (p_b \cdot p_{\nu_l}) [\hat{s} (q_{c(u)} \cdot p_l) + m_t^2 (q_g \cdot p_l)]}{\Lambda^2 ((\hat{s} - m_t^2)^2 + m_t^2 \Gamma_t^2) ((M_{l,\nu_l}^2 - M_W^2)^2 + M_W^2 \Gamma_W^2)}, \quad (4)$$

$p_{b,l,\nu_l}$  are the 4-momenta of the outgoing  $b$  quark, lepton, and neutrino respectively,  $q_{c(u),g}$  are the 4-momenta of the incoming charm(up) quark and gluon,  $\Gamma_W$  is the decay width of the  $W$  boson,

$$\Gamma_t = \Gamma_{t \rightarrow bW} \left[ 1 + \frac{128 M_W^2 \alpha_s}{3 \alpha_2 \left(1 - \frac{M_W^2}{m_t^2}\right)^2 \left(1 + 2 \frac{M_W^2}{m_t^2}\right)} \left(\frac{\kappa_{c(u)}}{\Lambda}\right)^2 \right] \quad (5)$$

is the decay width of the top quark, including the anomalous contribution for  $t \rightarrow cg$  (or  $t \rightarrow ug$ ),  $\Gamma_{t \rightarrow bW}$  is the standard model top quark decay width to a  $b$  quark and  $W$  boson,

$$M_{l,\nu_l}^2 \equiv (p_l + p_{\nu_l})^2 \quad (6)$$

is the invariant mass squared, not necessarily on shell, of the  $W$  boson, and  $\sqrt{\hat{s}}$  is the parton center of mass energy.

As mentioned earlier, we considered only the case which has a charged lepton (muon or electron) in the final state, to identify the  $W$  boson. Compared to the hadronic decay mode of the  $W$ , the background for these processes is smaller and the signal is not as hard to identify. In order to examine the kinematics of the decay products, we calculated the full three body phase space for the process, using the Breit-Wigner propagators to broaden the top quark and  $W$  boson distributions. Figure 2 shows the cross section at the Tevatron as a function of  $\kappa_c/\Lambda$ . In the top quark decay width, we included an additional term arising from  $t \rightarrow cg$ , as shown in Eq. (5). This term is proportional to  $|\kappa_c/\Lambda|^2$  and contributes significantly to the top quark width only if  $\kappa_c/\Lambda \gtrsim 0.2 \text{TeV}^{-1}$ . One can clearly see the effect of the additional channel for top quark decay, which decreases the  $t \rightarrow bW$  branching ratio and causes a noticeable deviation from quadratic behavior for  $\kappa_c/\Lambda \gtrsim 0.2 \text{TeV}^{-1}$ . The corresponding cross section for the t-u-g coupling has a similar shape, but is approximately an order of magnitude larger.

We calculated the  $p\bar{p}$  (for the Tevatron) and  $pp$  (for the LHC) cross sections for direct top production with the MRSA structure functions [16]. We have also examined the effect of using the CTEQ3M [17] structure functions. The difference between the two sets of structure functions is small. Several distributions were calculated, including the transverse momenta, the pseudorapidities, the jet separation, from the lepton, and the reconstructed  $\sqrt{\hat{s}}$ .

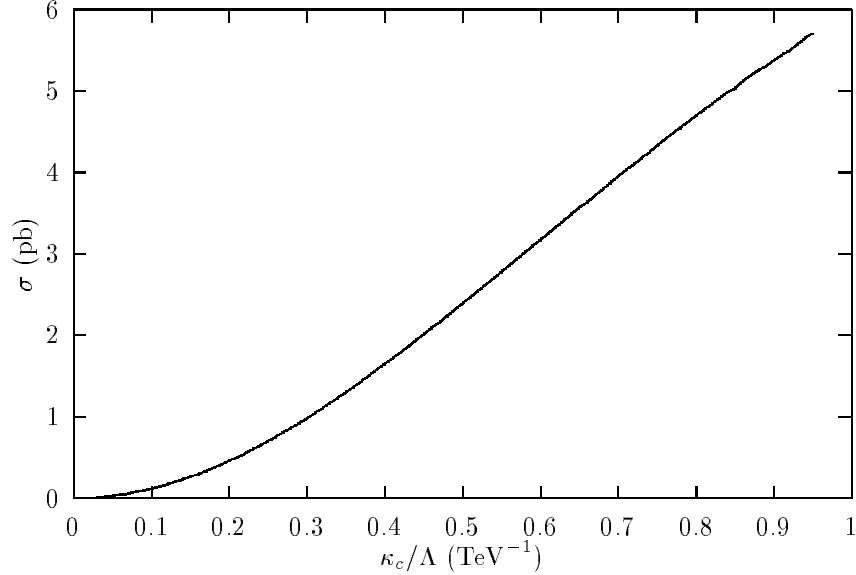


Figure 2: Direct top cross section vs.  $\kappa_c/\Lambda$  at Run 1 of the Tevatron.

In order to reduce the  $W + 1$  jet background, we made a series of cuts, which we will call the basic cuts, on the kinematic distributions. They are:

$$p_T(b, l, \nu_l) \geq 25 \text{ GeV} , \quad (7)$$

$$\eta_b \leq 2.0 , \quad (8)$$

$$\eta_l \leq 3.0 , \quad (9)$$

$$\Delta R \geq 0.4 , \quad (10)$$

where  $\eta_{b,l}$  are the pseudorapidities,  $\Delta R \equiv \sqrt{(\eta_b - \eta_l)^2 + (\phi_b - \phi_l)^2}$  is the separation between the b jet and the charged lepton in the detector, and  $\phi_{b,l}$  are the azimuthal angles. We also assumed a Gaussian smearing of the energy of the final state particles, given by:

$$\Delta E/E = 30\%/\sqrt{E} \oplus 1\% , \text{ for leptons} , \quad (11)$$

$$= 80\%/\sqrt{E} \oplus 5\% , \text{ for hadrons} , \quad (12)$$

where  $\oplus$  indicates that the energy dependent and independent terms are added in quadrature.

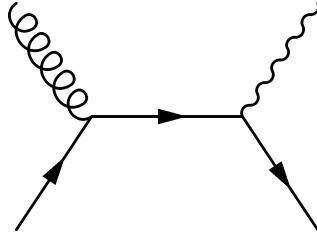


Figure 3: Sample tree level Feynmann diagram for  $W + 1jet$  production

To enhance the signal relative to the background, we want to make cuts on  $\sqrt{\hat{s}}$ , which should be sharply peaked at  $m_t$  for the signal. To experimentally determine  $\sqrt{\hat{s}}$ , one must reconstruct  $p_t = p_b + p_l + p_{\nu_l}$ . The neutrino is not observed, but its transverse momentum can be deduced from the missing transverse momentum. The longitudinal component of the neutrino momentum is determined by setting  $M_{l,\nu_l} = M_W$  in Eq. (6), and is given by:

$$p_L^{\nu_l} = \frac{\chi p_L^l \pm \sqrt{\vec{p}_T^2 (\chi^2 - p_{Tl}^2 p_{T\nu_l}^2)}}{p_{Tl}^2}, \quad (13)$$

where

$$\chi = \frac{M_W^2}{2} + \vec{p}_T^l \cdot \vec{p}_T^{\nu_l}, \quad (14)$$

and  $p_L$  and  $p_T$  refer to the longitudinal and transverse momenta respectively. Note that there is a two fold ambiguity in this determination. We chose the solution which would best reconstruct the mass of the top quark. In some rare cases, the quantity under the square root in Eq. (13) is negative. When this happened, we set this square root to zero, and used the corresponding result for the neutrino longitudinal momentum.

## Background Calculation

The main source of background to the direct top quark production is  $p\bar{p} \rightarrow W + 1 \text{ jet}$ . A sample tree level Feynmann diagram for this process is shown in Fig. 3. Another background process is standard model single top quark production when the associated jets are not observed. Examining the data presented in Ref. [18], we conclude that single top production is less than

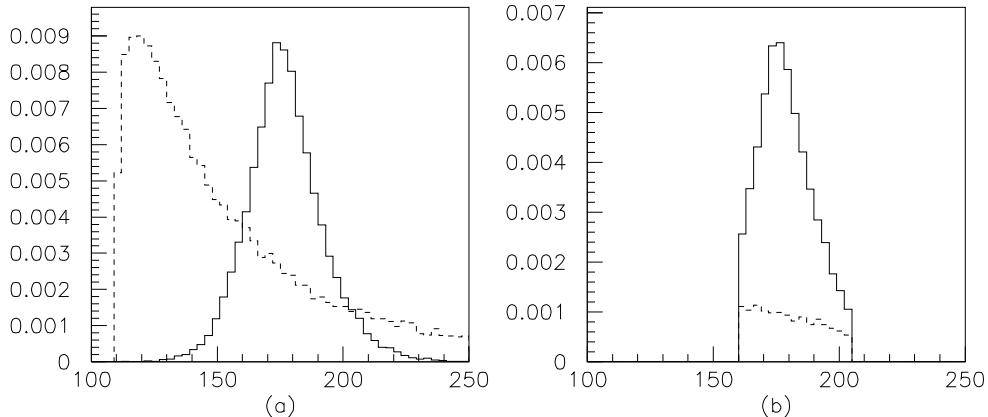


Figure 4:  $\sqrt{\hat{s}}$  distributions for the (a) basic and (b) optimized cuts without b-tagging at the upgraded Tevatron. The solid line represents the direct top production ( $\kappa_c/\Lambda = 0.2 \text{ TeV}^{-1}$ ). The dashed line is one thousandth of the  $W + 1$  jet background. The vertical axis is  $d\sigma/d\sqrt{\hat{s}}$  in pb/GeV, and the horizontal axis is  $\sqrt{\hat{s}}$  in GeV.

1% of the  $W + 1$  jet background when b-tagging is not used. When b-tagging reduces the  $W + 1$  jet background by a factor of 100, the single top background may be as large as 20% of the total background. However, since the discovery limit on  $\kappa/\Lambda$  scales as  $B^{-\frac{1}{4}}$  where  $B$  is the number of background events, a 20% change in the background affects the discovery limit by only 5%. We therefore ignore this background.

We used the VECBOS monte-carlo [20] to calculate the cross section for the  $W + 1$  jet background. We modified the program to produce the same distributions that were calculated for the signal, and applied the same basic cuts used in the signal calculation, Eqs. (7-10). To determine additional cuts which optimize the discovery limits on  $\kappa/\Lambda$ , we examined the kinematic distributions in  $\sqrt{\hat{s}}$ ,  $p_T$ ,  $\eta$ , and  $\Delta R$ . We found that three distributions,  $\sqrt{\hat{s}}$ ,  $p_{Tb}$ , and  $\eta_l$ , were most useful in isolating the signal from the background. These are shown in Figs. 4, 5, and 6, with the charm quark in the initial state and  $\kappa_c/\Lambda = 0.2 \text{ TeV}$  for the upgraded Tevatron. The solid lines represent direct top production, and the dashed lines represent the  $W + 1$  jet background divided by 1000. The cuts were optimized for each of four cases: Run 1 at the Tevatron with  $p\bar{p}$  collisions at  $\sqrt{s} = 1.8 \text{ TeV}$  and  $100 \text{ pb}^{-1}$  of data

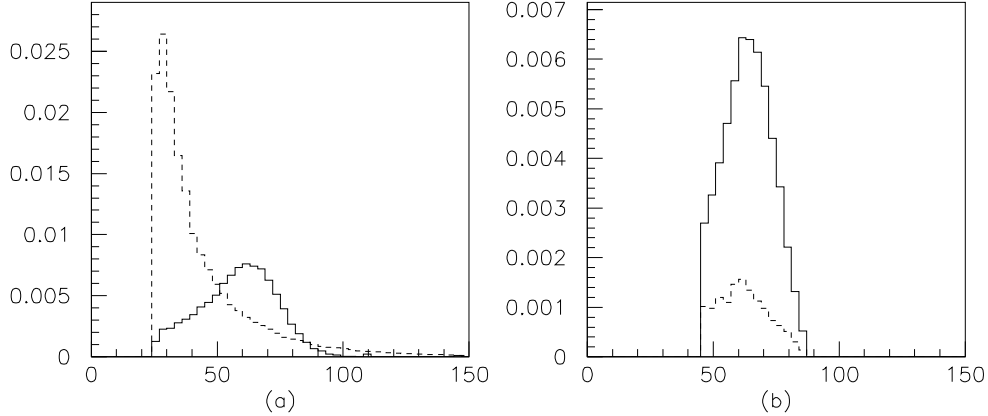


Figure 5:  $p_{Tb}$  distributions for the (a) basic and (b) optimized cuts without b-tagging at the upgraded Tevatron. The solid line represents the direct top production ( $\kappa_c/\Lambda = 0.2 \text{ TeV}^{-1}$ ). The dashed line is one thousandth of the  $W + 1$  jet background. The vertical axis is  $d\sigma/dp_{Tb}$  in pb/GeV, and the horizontal axis is  $p_{Tb}$  in GeV.

	$(p_{Tb})_{min}$	$(\sqrt{\hat{s}})_{min}$	$(\sqrt{\hat{s}})_{max}$	$(\eta)_{max}$
1.8 TeV Tevatron	35 GeV	155 GeV	205 GeV	1.8
2 TeV Tevatron	45 GeV	160 GeV	205 GeV	1.0
14 TeV LHC	35 GeV	165 GeV	195 GeV	1.0

Table 1: Optimized cuts for direct top quark production

per detector, Run 2 with  $\sqrt{s} = 2.0 \text{ TeV}$  and  $2 \text{ fb}^{-1}$ , Run 3 with  $2.0 \text{ TeV}$  and  $30 \text{ fb}^{-1}$ , and the LHC with  $pp$  collisions at  $14 \text{ TeV}$  and  $10 \text{ fb}^{-1}$ . The optimized cuts are shown in Table 1. The corresponding distributions with the up quark in the initial state are not shown; they have the same shape as for the charm quark, but are a factor of ten larger in magnitude, due to the much larger size of the valence up quark distribution in the initial state.

To further reduce the background, we assumed that silicone vertex tagging of the b jet would be available, with 36% efficiency at Run 1 of the Tevatron, and 60% at Runs 2 and 3, and at the LHC. In addition, we assumed that 1% of all non-b quark jets would be mistagged as b quark jets.



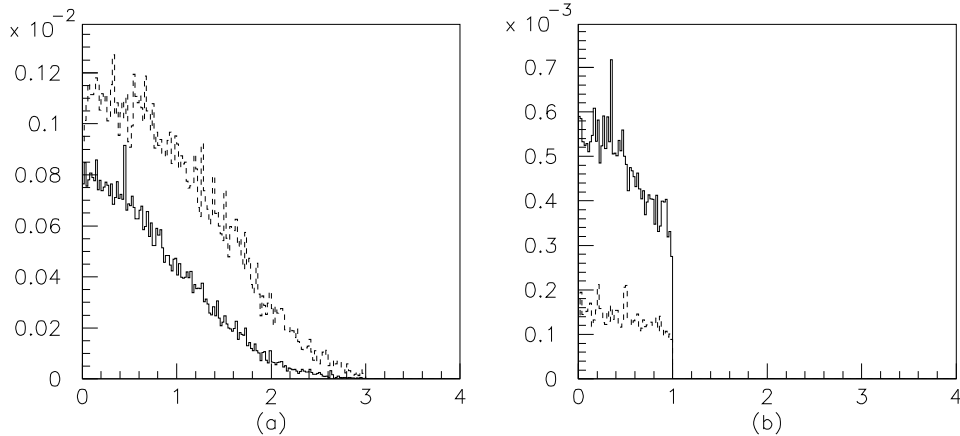


Figure 6:  $\eta_l$  distributions for the (a) basic and (b) optimized cuts without b-tagging at the upgraded Tevatron. The solid line represents the direct top production ( $\kappa_c/\Lambda = 0.2 \text{ TeV}^{-1}$ ). The dashed line is one thousandth of the  $W + 1$  jet background. The vertical axis is  $d\sigma/d\eta_l$  in pb, and the horizontal axis is  $\eta_l$ .

When b-tagging is present, if the jet produced is mistaken as a b jet, it remains a part of the background. The background can be reduced by a factor of 100 if the  $W + 1$  jet sample does not include a significant fraction of b quarks in the final state. It is possible to estimate the fraction of b quarks in the  $W + 1$  jet sample by taking the ratio  $|V_{cb}|^2/|V_{ud}|^2$  and multiplying by the ratio of the distribution fraction of charm quarks to up quarks in the proton ( $\approx 0.1$ ). We estimate that the fraction of b quark jets in the  $W + 1$  jet background is less than .03%, much less than the anticipated mistagging rate of 1%. We therefore ignore the possibility of having b quarks in the  $W + 1$  jet sample. Including b-tagging does not significantly affect the optimized cuts.

## Results and Discussion

We can use the results of the signal and background calculations to determine the minimum value of  $\kappa_c/\Lambda$  or  $\kappa_u/\Lambda$  observable at hadron colliders. Assuming Poisson statistics, the number of signal events (S) required for discovery of a

	$\sqrt{s}$	Luminosity	background	signal needed (fb)	
	TeV	$\text{fb}^{-1}$	fb	w/ b-tag	w/o b-tag
Run 1	1.8	0.1	19400	1370	190
Run 2	2.0	2	13000	245	27
Run 3	2.0	30	13000	63	6.4
LHC	14	10	79000	267	27

Table 2: Signal needed for the discovery of anomalous t-c-g and t-u-g couplings at the Tevatron and LHC at 95% confidence level. The background cross sections use the optimized cuts described in Table 1.

		Tevatron			LHC
		1.8 TeV	2 TeV		14 TeV
	b tagging?	$.1\text{fb}^{-1}$	$2\text{fb}^{-1}$	$30\text{fb}^{-1}$	$10\text{fb}^{-1}$
charm	no	.38	.14	.073	.020
	yes	.22	.062	.030	.0084
u quark	no	.096	.045	.023	.0081
	yes	.058	.019	.0094	.0033

Table 3: Discovery limits on  $\kappa_c/\Lambda$  and  $\kappa_u/\Lambda$  at the Tevatron and LHC. The results are reported in  $\text{TeV}^{-1}$

signal at the 95% confidence level is:

$$\frac{S}{\sqrt{S+B}} \geq 3, \quad (15)$$

where B is the number of background events obtained by multiplying the background cross section by the luminosity and dividing by 100 if b-tagging is present. The luminosity, background cross section, and signal cross section needed for discovery of anomalous flavor changing couplings is given in Table 2. The discovery limits may then be determined by comparing the signal calculation for a given  $\kappa/\Lambda$  to the signal needed, which can be obtained from Table 2. These discovery limits are shown in Table 3.

The results quoted in this paper all use the MRSA structure functions. When using the CTEQ3M structure functions, the direct top cross section increases by 15% when the charm quark coupling is used, corresponding to

a 7% improvement in the discovery limit for  $\kappa_c/\Lambda$ . This is primarily due to a larger charm quark density in the proton with the CTEQ3M structure functions. The  $W + 1$  jet cross section does not change significantly, nor does the direct top cross section when the up quark coupling is used.

We considered cases with and without b-tagging for each of the possibilities in Table 3. With the exception of Run 1 at the Tevatron, b-tagging improved the discovery limit on  $\kappa/\Lambda$  by 2.0 – 2.5 times. However, for the data from Run 1 at the Tevatron, b-tagging improves the discovery limit by only 40%. This is mostly due to less efficient b-tagging, and to the smaller number of events available with a lower luminosity.

In some single top quark production processes, there are regions of overlap between, for example,  $2 \rightarrow 1$  subprocesses and  $2 \rightarrow 2$  subprocesses. In particular, we worried about an overlap between the direct top production and the gluon fusion diagram in which one of the gluons is dissociated into a  $c\bar{c}$  pair, and the  $c$  combines with the other gluon to produce a top quark. Care must be taken with these processes to avoid double counting. A systematic method exists for calculating a subtraction term which solves this difficulty[18, 19]. The effect of the double counting is most significant if the initial state particles are massive. In the case of direct top quark production due to anomalous t-c-g or t-u-g couplings, the initial state particles are light enough that this does not significantly affect the overall cross section. We have therefore ignored this effect in our calculation.

Although the background due to single top quark production (a top quark with an associated jet) is small in the SM, there exists also the possibility for single top quark production with the anomalous t-c-g (or t-u-g) coupling, e.g. via  $q\bar{q} \rightarrow t\bar{c}$  ( $q\bar{q} \rightarrow t\bar{u}$ ). If the jet associated with the top quark is not seen, this would enhance the direct top signal due to the anomalous coupling. Therefore, the discovery limits quoted in Table 3 are conservative estimates of the level to which  $\kappa/\Lambda$  may be probed. A full treatment of single top production due to the anomalous t-c-g and t-u-g couplings will be considered elsewhere.

In conclusion, we have calculated the discovery limits for the anomalous chromomagnetic couplings t-c-g and t-u-g in hadron colliders using direct production of an s-channel top quark. We conservatively estimate that an anomalous charm quark coupling can be detected down to  $\kappa_c/\Lambda = .06 \text{ TeV}^{-1}$  at Run 2 of the Tevatron, and  $.009 \text{ TeV}^{-1}$  at the LHC. The cross section for the anomalous up quark coupling is larger, and we can measure  $\kappa_u/\Lambda$  down to  $0.02 \text{ TeV}^{-1}$  at Run 2 of the Tevatron, and  $0.003 \text{ TeV}^{-1}$  at the LHC. The

discovery limits for the upgraded Tevatron are approximately two (six) times better than those obtained in Ref. [15] for  $\kappa_c/\Lambda$  ( $\kappa_u/\Lambda$ ). The relative size of the direct top production and the anomalous top decay rate will help to differentiate the t-c-g and the t-u-g couplings.

Finally, we note that, in Ref [10], the authors found that electroweak-like corrections in a supersymmetric model can give  $\text{Br}(t \rightarrow cg)$  as large as  $1 \times 10^{-5}$  for the most favorable combinations of the parameters. In terms of our anomalous coupling parameter, this corresponds to  $\kappa_c/\Lambda = 0.0033$ . If supersymmetry is the only source for the anomalous t-c-g coupling, our calculations therefore indicate that future improvements at the LHC will be needed to make this a detectable signal, unless QCD-like corrections [9] further enhance the SUSY contributions, as discussed in Ref. [10].

## Acknowledgments

We would like to thank P. Baringer, J. Hauptman, A. Heinson, and X. Zhang for many useful discussions. This work was supported in part by the U.S. Department of Energy under Contract DE-FG02-94ER40817. M. Hosch was also supported under a GAANN fellowship.

## References

- [1] F. Abe et al., Phys.Rev.Lett.74 (1995) 2626.
- [2] S. Abachi et al., Phys.Rev.Lett.74 (1995) 2632.
- [3] J. Incandela, Nuovo Cim.109A (1996) 741.
- [4] Thomas J. LeCompte, FERMILAB-CONF-96-021-E (Jan 1996).
- [5] A.P. Heinson, FUTURE TOP PHYSICS AT THE TEVATRON AND LHC. In \*Les Arcs 1996, QCD and high energy hadronic interactions\* 43-52.
- [6] T. Han, K. Whisnant, B.L. Young and X. Zhang, UCD-96-07 (Mar 1996), to be published in Phys. Rev. D;  
K. Whisnant, Jin-Min Yang, Bing-Lin Young and X. Zhang, AMES-HET-97-1 (Feb 1997);  
R. Martinez and J-Alexis Rodriguez, Phys.Rev.D55 (1997) 3212;

- [7] D. Atwood, A. Kagan and T.G. Rizzo, Phys.Rev.D52 (1995). 6264;  
Douglas O. Carlson, Ehab Malkawi and C.P. Yuan, Phys.Lett.B337 (1994) 145;  
G.J. Gounaris, M. Kuroda and F.M. Renard, Phys.Rev.D54 (1996) 6861;  
G.J. Gounaris, J. Layssac, F.M. Renard, THES-TP-96-12 (Nov 1996).
- [8] B. Grzadkowski, J.F. Gunion and P. Krawczyk, Phys. Lett. B 268 (1991) 106;  
G. Eliam, J.L. Hewett and A. Soni, Phys. Rev. D44 (1991) 1473;  
M. Luke and M.J. Savage, Phys. Lett. B307 (1993) 387.
- [9] G. Couture, C. Hamzaoui and H. König, Phys. Rev. D52 (1995) 1713.
- [10] Jorge L. Lopez, D.V. Nanopoulos and Raghavan Rangarajan, ACT-05-97 (Feb 1997).
- [11] T.P. Cheng and M. Sher, Phys. Rev D48 (1987) 3484;  
W.S. Hou, Phys. Lett. B296 (1992) 179;  
L.J. Hall and S. Weinberg, Phys. Rev. D 48 (1993) 979;  
D. Atwood and A. Soni, SLAC-PUB-95-6927.
- [12] C.T. Hill, Phys. Lett. B266 (1991) 419, B 345 (1995) 483;  
B. Holdom, Phys Lett B339 (1994) 114, B351 (1995) 279.
- [13] H. Georgi, L. Kaplan, D. Morin and A. Schenk, Phys. Rev. D51 (1995) 3888;  
For a review of composite models, see, e.g., R.D. Peccei in: Proc. 1987 Lake Louise Winter Institute: Selected Topics in the Electroweak Interactions, eds. J.M. Cameron et al. (World Scientific, Singapore, 1987).
- [14] X. Zhang, Phys. Rev. D51 (1995) 5309;  
J. Berger, A. Blotz, H.-C. Kim and K Goeke, Phys. Rev. D54 (1996) 3598.
- [15] T. Han, K. Whisnant. B.-L. Young and X. Zhang, Phys. Lett. B385 (1996) 311.
- [16] A.D. Martin, R.G. Roberts and W.J. Stirling, Phys. Rev. D50 (1994) 6734.

- [17] H.L. Lai, J. Botts, J. Huston, J.G. Morfin, J.F. Owens, J. Qiu, W.K. Tung and H. Weerts; Phys. Rev. D51, 4763(1995).
- [18] A.P. Heinson, A.S. Belyaev and E.E. Boos, INP-MSU-96-41-448 (Dec 1996).
- [19] R.M. Barnett, H.E. Haber and D.E. Soper, Nucl. Phys. B306 (1988) 697;  
F. W. Olness and W.-K. Tung, Nucl. Phys. B308, (1988) 813.
- [20] F.A. Berends, H. Kuijf, B. Tausk and W.T. Giele, Nucl.Phys. B357 (1991) 32.